PERGAMON

Chemical Engineering Science 56 (2001) 1721–1729

Chemical Engineering Science

www.elsevier.nl/locate/ces

Dynamic behaviour of reactive distillation tray columns described with a nonequilibrium cell model

R. Baur[a,b], R. Taylor[b,c], R. Krishna[a,*]

[a]Department of Chemical Engineering, University of Amsterdam, Nieuwe Achtergracht 166, 1018 WV Amsterdam, Netherlands
[b]Department of Chemical Engineering, Clarkson University, Potsdam, NY 13699-5705, USA
[c]Department of Chemical Technology, University of Twente, 7500 AE Enschede, Netherlands

Abstract

In this paper we develop a generic, dynamic, nonequilibrium (NEQ) cell model for reactive distillation (RD) tray columns. The features of our model are (1) the use of Maxwell–Stefan equations for describing mass transfer between fluid phases, (2) the reaction is assumed to take place in the liquid phase, both within the diffusion layer and in the bulk, (3) the coupling between mass transfer and chemical reactions within the diffusion layer is accounted for, and (4) the use of multiple well-mixed cells in the liquid and vapour flow directions in order to account for staging in either fluid phase. The utility of the developed model is demonstrated by carrying out simulations of a RD column for production of ethylene glycol (EG) by hydration of ethylene oxide. The introduction of staging in the vapour and liquid phases improves the conversion to EG and also reduces the formation of the unwanted di-ethylene glycol. Furthermore, there are marked differences between the dynamic column response to feed perturbations between the developed NEQ model and the more commonly used equilibrium (EQ) stage model.

Keywords: Reactive distillation; Equilibrium stage model; Nonequilibrium stage model; Dynamics; Maxwell–Stefan equations; Ethylene glycol

1. Introduction

To describe the dynamics of reactive distillation (RD) columns, three types of models exist in the literature.

(1) Equilibrium (EQ) stage model (Abufares & Douglas, 1995; Bartlett & Wahnschafft, 1998; Espinosa, Martinez, & Perez, 1994; Grosser, Doherty, & Malone, 1987; Kumar & Daoutidis, 1999; Moe, Hauan, Lien, & Hertzberg, 1995; Perez-Cisneros, Schenk, Gani, & Pilavachi, 1996; Scenna, Ruiz, & Benz, 1998; Schrans, de Wolf, & Baur, 1996; Sneesby, Tadé, & Smith, 1998),
(2) EQ stage model with fixed stage efficiencies (Alejski & Duprat, 1996; Ruiz, Basualdo, & Scenna, 1995), and
(3) Nonequilibrium (NEQ) stage model (Kreul, Gorak, Dittrich, & Barton, 1998).

Roat, Downs, Vogel, and Doss (1986) integrate the control system equations with the EQ stage model equations and show, using the Eastman methyl acetate process, that control schemes with good steady-state characteristics may fail under unsteady-state conditions. Besides the methyl acetate process, there are other RD processes such as the synthesis of ethylene glycol that are carried out in tray columns in which the contacting pattern on any stage is cross-current. For large diameter columns used in industry there will be sufficient staging in both the vapour and liquid phases. Liquid phase staging is considerably more important for RD operations than for conventional distillation because of its influence on conversion and selectivity. The assumption of well-mixed vapour and liquid phases, made in all published EQ and NEQ models, does not hold for such RD tray columns. The primary objective of our paper is to develop a rigorous dynamic NEQ model for RD columns, which would cater for cross-flow contacting of vapour and liquid phases by dividing the stage into a number of well-mixed cells in the liquid and vapour flow directions. We demonstrate the utility of our developed NEQ cell model by performing simulations of

* Corresponding author. Tel.: +31-20-525-7007; fax: +31-20-525-5604.
E-mail address: krishna@its.chem.uva.nl (R. Krishna).

0009-2509/01/$ - see front matter
PII: S0009-2509(00)00401-2

a column for production of ethylene glycol by hydration of ethylene oxide.

2. Nonequilibrium (NEQ) cell model development

The basic idea of the NEQ cell model for RD tray columns is shown in Fig. 1. Each stage is divided into a number of *contacting cells*; these cells describe just a small section of the tray. The vapour entering a stage is divided equally into the number of cells, m in total, in the horizontal row. The liquid entering the stage is similarly divided equally between the number of cells, n in total, in a vertical column. The feed entering the stage is also apportioned in the same manner to the entering row, or column, of cells in the same manner. By choosing an appropriate number of cells in each flow direction, one can model the actual flow patterns on a tray. A column of cells can model plug flow in the vapour phase, and multiple columns of cells can model plug flow in the liquid phase. When the number of well-mixed cells in any flow direction is four or more, we have essentially plug flow of that phase. Various degrees of backmixing in the vapour and liquid phases can be modelled by choosing the number of well-mixed cells to lie between one and say four. The precise estimate of the number of cells may be derived from eddy diffusion models for trays (Bennett & Grimm, 1991). Further details of the implementation of the cell model can be found in Higler, Taylor and Krishna (1999) and Higler, Krishna and Taylor (1999) who have presented the steady-state version of the cell model for RD columns. We first analyse the conservation relations for a typical cell on a tray (cf. Fig. 1(b)); the complete set of model equations is presented in Table 1.

The dynamics of a well-mixed cell is determined, inter alia, by the storage capacity, or accumulation, of mass and energy in the vapour and liquid phase. The time rate of change of the number of moles of component i in the vapour (M_i^V) and liquid (M_i^L), is given by Eq. (1). A total of r (homogeneous) chemical reactions takes place in the liquid phase with a reaction rate R_k and ε^L represents the volumetric liquid hold-up in the cell. Heterogeneous chemical reactions taking place inside catalyst particles are taken account with a pseudo-homogeneous description using catalyst effectiveness factors and effective reaction rate constants. Higler, Krishna and Taylor (2000) have developed a nonequilibrium model for RD columns taking intraparticle transport into account.

The overall molar balance for the cell, Eq. (2), is obtained by summing Eq. (1) over the total number of components, c in the mixture. The mole fractions of the vapour and liquid phases are calculated from the respective phase molar hold-ups; see Eq. (3). Only $c-1$ of these mole fractions are independent because the phase mole fractions sum to unity; see Eq. (4). In our model $c-1$ molar component balances (1) have been implemented along with Eqs. (2)–(4).

The phase energy balance is written in terms of the energy "hold-ups" in the cell; see Eq. (5). The heat removal from the liquid phase in each cell is just heat removal from the stage divided by the total number of cells, i.e. $Q^L = Q_j^L/(m \times n)$. An analogous equation holds

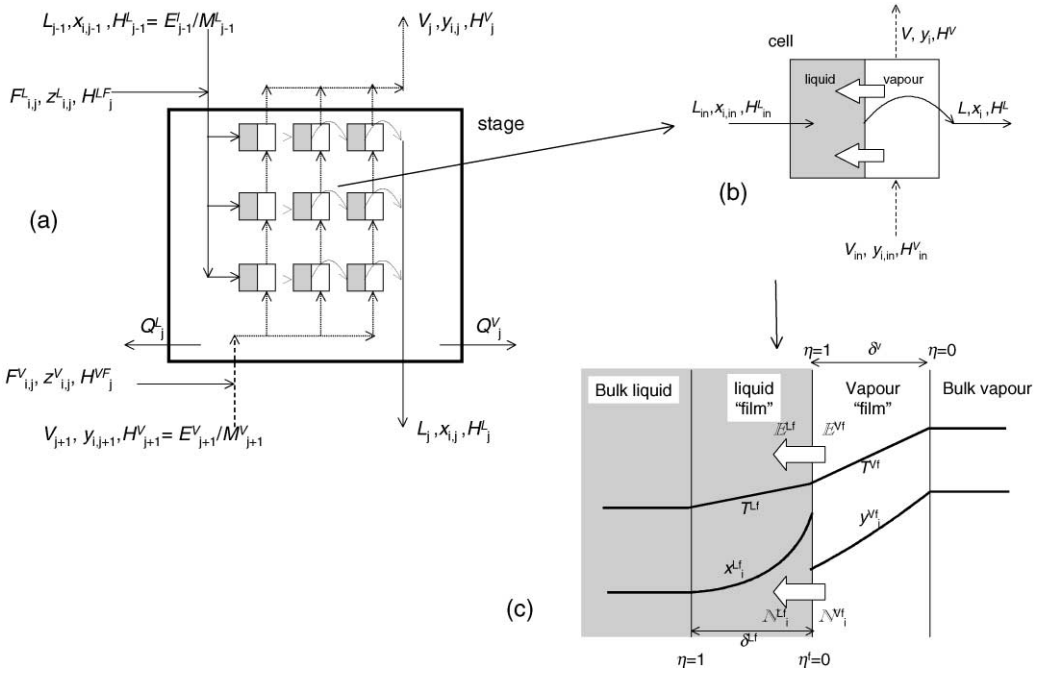

Fig. 1. (a) Schematic representation of a NEQ cell model for a stage j, (b) balance relations for a representative cell, (c) composition and temperature profiles within the vapour and liquid "films".

Table 1
Equations describing dynamic NEQ cell model

Equation type and number	Liquid phase	Vapour phase
Equations describing conservation laws for NEQ cell		
Molar component balance, Eq. (1)	$\frac{dM_i^L}{dt} = L_{in}x_{i,in} - Lx_i + \mathbb{N}_i^L + \sum_{k=1}^{r} v_{i,k}R_k\varepsilon^L$	$\frac{dM_i^V}{dt} = V_{in}y_{i,in} - Vy_i - \mathbb{N}_i^V$
Total molar hold-up, Eq. (2)	$\frac{dM^L}{dt} = L_{in} - L + \sum_{k=1}^{c}\mathbb{N}_i^L + \sum_{i=1}^{c}\sum_{k=1}^{r} v_{i,k}R_k\varepsilon^L$	$\frac{dM^V}{dt} = V_{in} - V - \sum_{k=1}^{c}\mathbb{N}_k^V$
Mole fractions, Eq. (3)	$x_i = M_i^L/M^L$	$y_i = M_i^V/M^V$
Summation, Eq. (4)	$\sum_{k=1}^{c} x_k = 1$	$\sum_{k=1}^{c} y_k = 1$
Energy balance, Eq. (5)	$\frac{dE^L}{dt} = L_{in}\frac{E_{in}^L}{M_{in}^L} - L\frac{E^L}{M^L} + \mathbb{E}^L - Q^L$	$\frac{dE^V}{dt} = V_{in}\frac{E_{in}^V}{M_{in}^V} - V\frac{E^V}{M^V} - \mathbb{E}^V - Q^V$
Energy hold-up, Eq. (6)	$E^L = H^L M^L$	$E^V = H^V M^V$
Equations describing conservation laws within diffusion "films"		
Molar component balance, Eq. (7)	$\frac{\partial\mathbb{N}_i^{Lf}(\eta^{Lf})}{\partial\eta^{Lf}} + \sum_{k=1}^{r} v_{i,k}R_k(\eta^{Lf})A\delta^{Lf} = 0$	$\frac{\partial\mathbb{N}_i^{Vf}(\eta^{Vf})}{\partial\eta^{Vf}} = 0$
Maxwell–Stefan relations, Eq. (8)	$\frac{x_i^{Lf}}{\mathbb{R}T^{Lf}}\frac{\partial\mu_i^{Lf}}{\partial\eta} = \sum_{k=1}^{c}\frac{x_i^{LF}\mathbb{N}_k^{Lf} - x_k^{LF}\mathbb{N}_i^{Lf}}{c_t^{Lf}\kappa_{i,k}^{Lf}A}$	$\frac{y_i^{Vf}}{\mathbb{R}T^{Vf}}\frac{\partial\mu_i^{Vf}}{\partial\eta} = \sum_{k=1}^{c}\frac{y_i^{Vf}\mathbb{N}_k^{Vf} - y_k^{VF}\mathbb{N}_i^{Vf}}{c_t^{Vf}\kappa_{i,k}^{Vf}A}$
Summation equations, Eq. (9)	$\sum_{k=1}^{c} x_{i,j}^{Lf} = 1$	$\sum_{k=1}^{c} y_{i,j}^{Vf} = 1$
Energy balance, Eq. (10)	$\frac{\partial\mathbb{E}^{Lf}}{\partial\eta^{Lf}} = 0$	$\frac{\partial\mathbb{E}^{Vf}}{\partial\eta^{Vf}} = 0$
Energy transfer rate, Eq. (11)	$\mathbb{E}^{Lf} = -h^{Lf}A\frac{\partial T^{Lf}}{\partial\eta} + \sum_{i=1}^{c}\mathbb{N}_i^{Lf}H_i^{Lf}$	$\mathbb{E}^{Vf} = -h^{Vf}A\frac{\partial T^{Vf}}{\partial\eta} + \sum_{i=1}^{c}\mathbb{N}_i^{Vf}H_i^{Vf}$
Relations at interface between vapour and liquid for cell		
Vapour–liquid Equilibrium, Eq. (12)	$K_i x_i\|_I = y_i\|_I$	
Temperature equilibrium, Eq. (13)	$T^{Lf}\|_I = T^{Vf}\|_I$	
Continuity of molar fluxes, Eq. (14)	$\mathbb{N}_i^{Lf}\|_I = \mathbb{N}_i^{Vf}\|_I$	
Continuity of energy fluxes, Eq. (15)	$\mathbb{E}^{Lf}\|_I = \mathbb{E}^{Vf}\|_I$	
Inter-relation between stage parameters and cell parameters		
Molar flows leaving stage, Eq. (16)	$\sum_{nn=1}^{n} L_{m,nn} = L_j$	$\sum_{mm=1}^{m} V_{mm,n} = V_j$
Mole fractions of flows leaving stage, Eq. (17)	$\sum_{nn=1}^{n} x_{i,m,nn}L_{m,nn} = x_{i,j}L_j$	$\sum_{mm=1}^{m} y_{i,mm,n}V_{mm,n} = y_{i,j}V_j$
Enthalpy of flows leaving stage, Eq. (18)	$\sum_{nn=1}^{n}\frac{E_{m,nn}^L}{M_{m,nn}^L}L_{m,nn} = H_j^L L_j$	$\sum_{mm=1}^{m}\frac{E_{mm,n}^V}{M_{mm,n}^V}V_{mm,n} = H_j^V V_j$
Volumetric hold-up, Eq. (19)	$(m\times n)\varepsilon^L = \varepsilon_j^L$	$(m\times n)\varepsilon^V = \varepsilon_j^V$
Hydrodynamics of trays		
Calculation of volumetric liquid and vapour hold-ups, Eq. (20)	$\frac{1}{c_{t,j}^L}M_j^L \equiv \varepsilon_j^L = h_{\mathrm{cl},j}A_{\mathrm{bub},j}$	$\frac{1}{c_{t,j}^V}M_j^V \equiv \varepsilon_j^V = (h_t - h_{\mathrm{cl},j})A_{\mathrm{bub},j}$

for the vapour phase. The energy hold-ups are related to the corresponding molar hold-ups via the stage enthalpies by Eq. (6). There is no need to take separate account in Eq. (6) of the heat generated due to chemical reaction since the computed enthalpies include the heats of formation. The phase temperatures T^V and T^L are determined from the corresponding phase enthalpies using an ideal or excess enthalpy model.

The resistance to mass and energy transfer is located in thin "films" adjacent to the vapour–liquid interface; see Fig. 1(c). The liquid-phase diffusion film thickness δ^{Lf} is of the order of 10 μm and the vapour-phase diffusion film thickness δ^{Vf} is of the order of 100 μm. The storage capacity for mass and energy in these films is negligibly small compared to that in the bulk fluid phases and so the interfacial transfer rates can be calculated from quasi-stationary interfacial transfer relations. The molar component balance within the film is given by Eq. (7) where A represents the interfacial area and $A\delta^{Lf}$ represents the volume available for liquid-phase chemical reaction. The coupling of diffusion and chemical reaction within the liquid film is particularly important for fast chemical reactions (Hatta number exceeding unity). The molar transfer rate $\mathbb{N}_i$ is related to the chemical potential gradients by the Maxwell–Stefan equations (Krishna & Wesselingh, 1997; Taylor & Krishna, 2000); see Eq. (8). The $\kappa_{i,k}$ represents the mass transfer coefficient of the $i-k$ pair in the phase; this coefficient is estimated from information on the corresponding Maxwell–Stefan diffusivity $Đ_{I,k}$ using the standard procedures discussed in Taylor and Krishna (1993). Only $c-1$ of Eqs. (8) are independent. The summation Eq. (9) holds. The energy balance within the diffusion film is given by Eq. (9), where the interfacial energy transfer rate $\mathbb{E}$ has both conductive and convective contributions; see Eq. (11). At the vapour–liquid interface we assume phase equilibrium described by Eqs. (12) and (13). Furthermore, the fluxes of mass and energy are continuous across the interface (cf. Eqs. (14) and (15)).

The link between the cell parameters and the stage parameters is given by Eqs. (16)–(19) of Table 1. The sum of the molar liquid flows leaving the last column of cells gives the total molar liquid flow leaving the stage j; see Eq. (16). A corresponding equation holds for the vapour flows leaving the top row of cells. The volumetric hold-ups per cell are simply a fraction $1/(m \times n)$ of the corresponding stage hold-ups; see Eq. (19). A similar relation holds for the interfacial area. Phase equilibrium and reaction rates are calculated per cell based on the local compositions and temperature prevailing. Hydrodynamics and mass transfer parameters are calculated using stage flows, compositions and temperatures. For example, for sieve tray columns the volumetric liquid hold-up on the stage can be calculated from knowledge of the active (or bubbling) tray area, A_{bub}, and estimation of the clear liquid height, h_{cl} (Bennett, Agrawal, & Cook, 1983; Barker & Self, 1962). From the chosen tray spacing the corresponding volumetric vapour hold-up can be calculated (cf. Eq. (20)). The liquid and vapour residence times can be calculated from a knowledge of the volumetric hold-ups and flows on the stage. Interested readers can download the technical manual from our website: http://www.clarkson.edu/ ~ chengweb/faculty/taylor/chemsep/chemsep.html, which contains in detail all thermodynamics, hydrodynamics and mass transfer models for tray columns which have been implemented in our reactive distillation software. The code for these models represents a large fraction of the overall program size.

The liquid hold-up in the reboiler and condenser is usually much larger than the hold-up on a particular stage. High liquid hold-ups lead to operational robustness, but also cause the equations to be very stiff. In our model implementation, liquid buffers are incorporated at the top and bottom. The partial, or total, condenser is followed by a reflux drum buffering the condensate. A partial condenser is modelled as an equilibrium stage. The reflux drum is considered to be a well-mixed system with a specified volumetric capacity. The mean liquid residence time and dynamic characteristics are, therefore, fully determined with this specification. The liquid leaving the bottom of the column is led to a reboiler drum with a specified volumetric capacity (hold-up) and assumed to be well mixed. The contents are then transferred to a partial, or total reboiler. A partial reboiler is modelled as an equilibrium stage.

The differential equations that describe mass transfer through the vapour and liquid films are discretised over the film thickness by application of a finite difference scheme, with fixed grid points. The resulting set of differential–algebraic equations is solved using the DAE solver BESIRK (Kooijman, 1995; Kooijman & Taylor, 1995).

3. Ethylene glycol case study

We consider the reaction of ethylene oxide (EO) with water to produce ethylene glycol (EG) in a reactive distillation column. The reaction is irreversible and proceeds in the presence of a catalyst: $\mathrm{EO} + \mathrm{H_2O} \rightarrow \mathrm{EG}$. In addition we have an unwanted side reaction in which ethylene glycol reacts with ethylene oxide to form di-ethyleneglycol ($\mathrm{EO} + \mathrm{EG} \rightarrow \mathrm{DEG}$). The reaction rate constant of the second reaction is, under reaction conditions, about three times as large as the rate constant of the first reaction. Therefore, in a conventional reactor with equimolar feed, a considerable amount of DEG is produced. Furthermore, the reactions are both highly exothermic requiring good temperature control. A reactive distillation column offers both the advantages of heat integration and in situ separation of the desired product, EG, preventing further reaction to DEG. By choosing total reflux operation, one can ensure that water mole fraction in the liquid phase on all the trays in the reactive section is close to unity (EO is considerably more volatile than water). The ethylene oxide that is supplied to the column reacts with water to form EG and because of the high surplus of water in the liquid, the concentrations of EO and EG will be very low. This results in a low production rate of DEG. Furthermore, the distillation

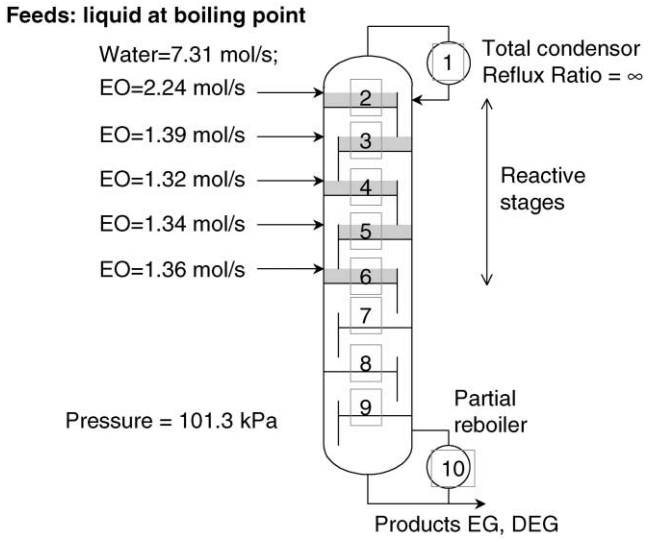

Fig. 2. Configuration of RD column for hydration of ethylene oxide to ethylene glycol. Further details to be found in Ciric and Miao (1994) and Baur et al. (2000).

process provides direct temperature control, since the temperature of the liquid phases will always be at the boiling point. Hot spot formation and the danger of runaway reactions are non-existent in reactive distillation.

The column configuration chosen for case study is similar to the set up of Ciric and co-workers (Ciric & Gu, 1994; Ciric & Miao, 1994), details of which are given in Fig. 2. This is a 10-stage sieve tray column (including total condenser and partial reboiler). Water is supplied to the top of the column, while the EO feed is distributed along the top section of the column. Reactions are assumed to take place only on stages 2–6 because catalyst is considered to be present only on these stages. The column is operated at total reflux, while in the bottom a boilup ratio of 24 is maintained. The reaction kinetics and thermodynamics data are the same as those reported in the paper by Ciric and Miao (1994). Since the NEQ model calculations require the estimation of heat and mass transfer coefficients, we need to specify the tray configuration and layout. The configuration of the sieve trays is the same as in our early study of steady-state operation (Baur, Higler, Taylor & Krishna, 2000): column diameter = 1.7 m; total tray area = 2.27 m^2; number of liquid flow passes = 1; tray spacing = 0.7 m; liquid flow path length = 1.283 m; fractional active (bubbling) area = 0.86; fractional hole area = 0.0858; fractional downcomer area = 0.07; hole diameter = 4.5 mm; weir height = 80 mm; total weir length = 1.52 m; weir type = segmental; downcomer clearance = 0.01 m; tray deck thickness = 25 mm. The volumetric liquid hold-up in the reflux drum is 700 l and in the reboiler is 1500 l.

The dynamic simulations were performed as follows. The earlier developed steady-state version of the NEQ model (Baur et al., 2000) was first used to determine the steady-state conditions. Using this steady-state solution as a starting basis, the simulations were run in the dynamic mode and at $t = 1$ h, disturbances in the feed flows of EO or H_2O are introduced to study the column response. These disturbances lasted for 1 h.

Let us first consider the influence of the reboiler and condenser hold-ups on the column responses. Simulations using the NEQ cell model taking $m = 1$, $n = 1$ are shown in Fig. 3 for a 10% increase in the water feed to stage 2. Increased buffer capacities (1300 and 2300 l in condenser and reboiler) leads to a slower approach to steady state than for the base case configuration (700 l condenser and 1500 l reboiler). However, we note the higher under-shoots in the temperature and mole fractions of EG and DEG in the bottom product stream with

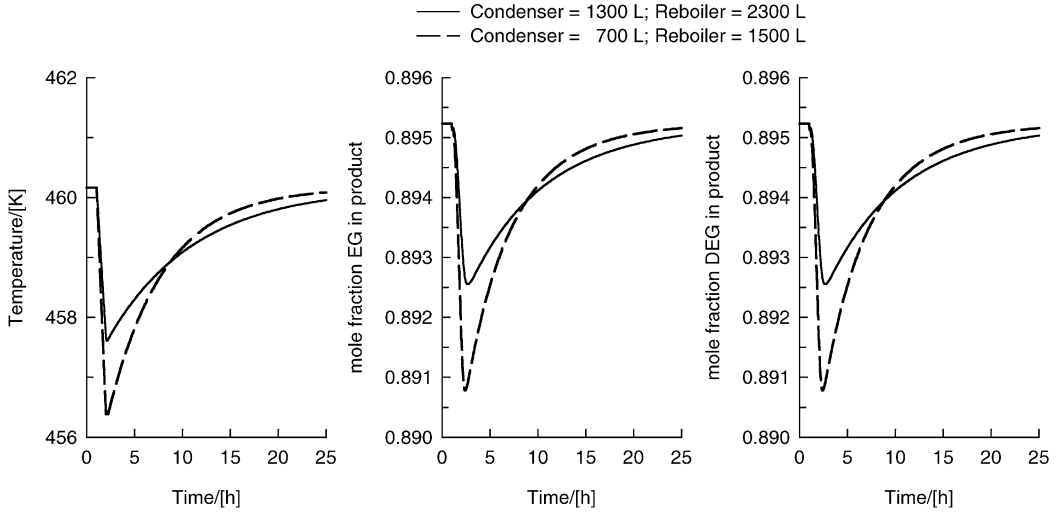

Fig. 3. Dynamic response to a 10% increase in the water feed flow to stage 2, 1 h after column start-up. Number of cells in vapour and liquid flow directions are $m = 1$, $n = 1$.

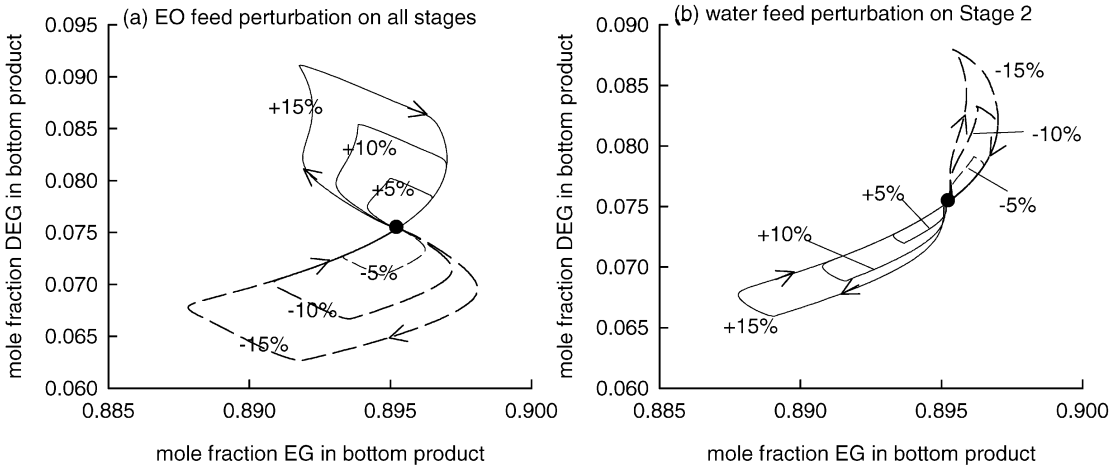

Fig. 4. Composition phase portraits obtained during feed perturbations of EO (to all stages 2–6) and H_2O (to stage 2) to various extents, 1 h after column start-up. Number of cells in vapour and liquid flow directions are $m = 1$, $n = 1$. The large black dot represents the initial (and final) steady state. The arrows indicate the direction of the transient composition trajectories.

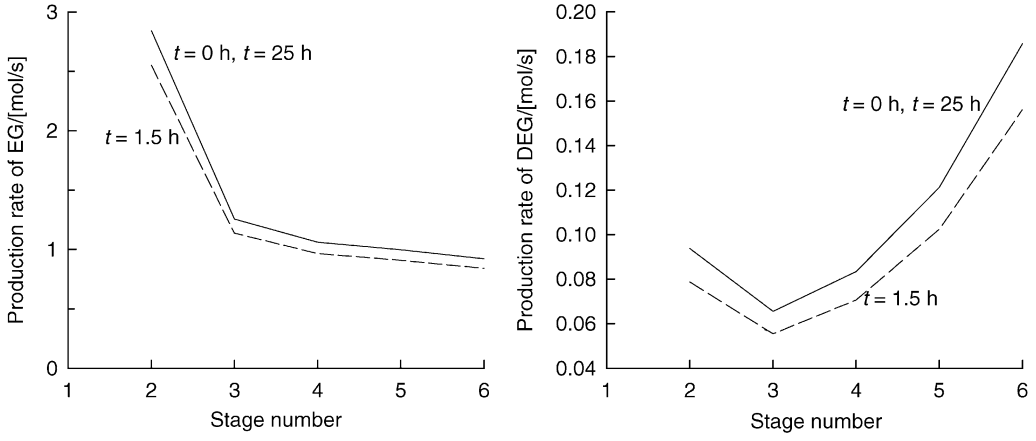

Fig. 5. Production rates of EG and DEG along the reactive stages at time $t = 0$ and 1.5 h. Response to a -10% perturbation of EO feed to all reactive stages. NEQ model with $m = 1$ and $n = 1$.

lower buffer capacities. All other simulations reported below are with the base case buffer capacities.

Fig. 4 shows the dynamic composition phase portrait (DEG vs. EG mole fractions in the bottom product) obtained after perturbations in the EO and H_2O feed flows to various extents. A positive EO perturbation feed leads to substantial unwanted DEG production during the transience. Similarly, a positive H_2O feed perturbation has the opposite, beneficial, effect. It is interesting to note that the all feed perturbations lead to substantial changes in the DEG composition and have only a minor influence on the EG product composition. This point is further emphasised in Fig. 5 which shows the production rates of EG and DEG on the reactive stages for a -10% perturbation to EO feed on stages 2–6. It is interesting to note the significant decrease in the DEG production rate on all stages during transience (see the reaction rate profiles at $t = 1.5$ h after start-up). This decrease in DEG production rate is more pronounced than the decrease in the EG production rate. A proper control of feed flows is, therefore, essential to preserve reaction selectivity in the column.

For the 1.7 m diameter column, with a weir height of 80 mm, existing correlations would anticipate a substantial degree of staging in the liquid and vapour phases. In Fig. 6, we compare the transient responses to a 10% decrease in the EO feed (to all reactive stages) for three cases: (1) NEQ cell model with 1×1 cells, (2) NEQ cell model with 4×4 cells (which would correspond roughly with plug flow of both phases on a tray), and (3) EQ model. As anticipated, the EQ model anticipates the best RD performance with respect to conversion and selectivity, i.e. the highest EG and the lowest DEG composition in the bottom product. The 4×4 cell NEQ model is

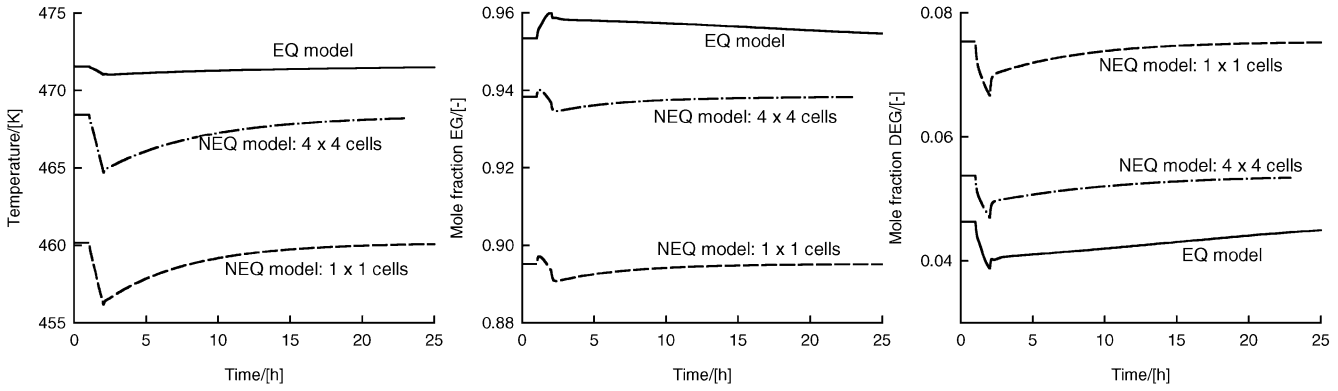

Fig. 6. Dynamic responses of the temperature, EG mole fraction, DEG mole fraction of the bottom product stream to a 10% decrease in the EO feed flow (to stages 2–6), 1 h after column start-up. Comparison of NEQ cell models ($m = 1$, $n = 1$ and $m = 4$, $n = 4$) with EQ model.

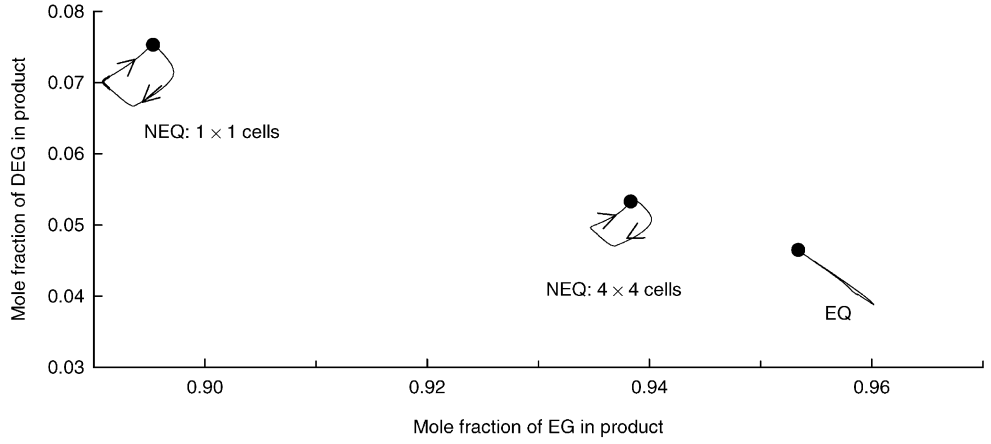

Fig. 7. Composition phase portraits (DEG vs. EG composition in bottom product) during transient response to a 10% decrease in the EO feed flow (to stages 2–6), 1 h after column start-up. Comparison of NEQ cell models ($m = 1$, $n = 1$ and $m = 4$, $n = 4$) with EQ model. The large black dots denote the initial (and final) steady state values.

considerably superior to the 1×1 cell NEQ model in this respect. The corresponding composition phase portraits in Fig. 7 illustrate this more clearly. The EQ model covers a much smaller composition space during transience than either of the two NEQ cell models.

4. Concluding remarks

We have developed a rigorous dynamic NEQ cell model for RD columns to account for realistic contacting of the vapour and liquid phases on a tray. With the aid of a case study for production of ethylene glycol we have underlined the importance of staging in the vapour and liquid phases on the conversion to EG and on the formation of the by-product DEG. Feed flow perturbations affect by-product formation to a significant extent. The dynamic EQ model, widely used in the literature, shows much less sensitivity to disturbances. It is concluded that for proper description of the RD tray column dynamics, the NEQ cell model is essential.

Notation

a	interfacial area per unit volume, m^{-1}
A	interfacial area, m^2
A_{bub}	active (bubbling) area on tray, m^2
c	number of components in the mixture
c_t	total concentration, mol/m^3
$D_{i,k}$	Maxwell–Stefan diffusivity, m^2/s
$\mathbb{E}$	energy transfer rate, J/s
F	Feed stream, mol/s
h_{cl}	clear liquid height, m
h_t	tray spacing, m
h_w	weir height, m
H	molar enthalpy, J/mol
h	heat transfer coefficient, $W/m^2/K$

K vapour–liquid equilibrium constant
L liquid flow rate, mol/s
m number of cells along the liquid flow direction
M_i molar hold-up of component i, mol
n number of cells along the vapour flow direction
$\mathbb{N}$ mass transfer rate, mol/s
Q heat duty, J/s
r number of reactions
$R_{i,j}$ reaction rate, mol/m^3/s
$\mathbb{R}$ gas constant, J/mol/K
T temperature, K
V vapour flow rate, mol/s
W weir length, m
x mole fraction in the liquid phase
y mole fraction in the vapour phase
z mole fraction in the feed stream

Greek letters
ε volumetric hold-up of phase, m^3
δ diffusion film thickness, m
η dimensionless coordinate
κ mass transfer coefficient, m/s
μ Chemical potential, J/mol

Subscripts
i component index
in stream entering cell
j stage index
I referring to interface
k index
mm index for cells in a row
nn index for cells in a column
t total

Superscripts
F referring to feed stream
L referring to liquid phase
Lf referring to liquid diffusion film
V referring to vapour phase
Vf referring to vapour diffusion film

Acknowledgements

Partial support for our work comes from BP-Amoco Chemicals. RK and RB acknowledge financial support from the Netherlands Organisation for Scientific Research (NWO) in the form of a "programmasubsidie" for research on reactive separations.

References

Abufares, A. A., & Douglas, P. L. (1995). Mathematical modeling and simulation of an MTBE catalytic distillation process using SPEEDUP and AspenPlus. *Chemical Engineering Research and Design, Transactions of the Institution of Chemical Engineers, Part A*, *73*, 3–12.

Alejski, K., & Duprat, F. (1996). Dynamic simulation of the multicomponent reactive distillation. *Chemical Engineering Science*, *51*, 4237–4252.

Barker, P. E., & Self, M. F. (1962). The evaluation of liquid mixing effects on a sieve plate using unsteady and steady-state tracer techniques. *Chemical Engineering Science*, *17*, 541–554.

Bartlett, D. A., & Wahnschafft, O. M. (1998). Dynamic simulation and control strategy evaluation for MTBE reactive distillation. In: J. F. Pekny & G. E. Blau (Eds.), *Foundations of computer-aided process operation*, American Institute of Chemical Engineers Symposium Series, vol. 320 (pp. 315–321). New York: A.I.Ch.E.

Baur, R., Higler, A. P., Taylor, R., & Krishna, R. (2000). Comparison of equilibrium stage and nonequilibrium stage models for reactive distillation. *Chemical Engineering Journal*, *76*, 33–47.

Bennett, D. L., Agrawal, R., & Cook, P. J. (1983). New pressure drop correlation for sieve tray distillation columns. *American Institute of Chemical Engineers Journal*, *29*, 434–442.

Bennett, D. L., & Grimm, H. J. (1991). Eddy diffusivity for distillation sieve trays. *American Institute of Chemical Engineers Journal*, *37*, 589–596.

Ciric, A. R., & Gu, D. (1994). Synthesis of nonequilibrium reactive distillation by MINLP optimization. *American Institute of Chemical Engineers Journal*, *40*, 1479–1487.

Ciric, A. R., & Miao, P. (1994). Steady-state multiplicities in an ethylene glycol reactive distillation column. *Industrial and Engineering Chemistry Research*, *33*, 2738–2748.

Espinosa, J., Martinez, E., & Perez, G. A. (1994). Dynamic behavior of reactive distillation columns, Equilibrium systems. *Chemical Engineering Communications*, *128*, 19–42.

Grosser, J. H., Doherty, M. F., & Malone, M. F. (1987). Modeling of reactive distillation systems. *Industrial and Engineering Chemistry Research*, *26*, 983–989.

Higler, A., Krishna, R., & Taylor, R. (1999). A nonequilibrium cell model for multicomponent (reactive) separation processes. *American Institute of Chemical Engineers Journal*, *45*, 2357–2370.

Higler, A., Krishna, R., & Taylor, R. (2000). Non-equilibrium modelling of reactive distillation: A dusty fluid model for heterogeneously catalysed processes. *Industrial and Engineering Chemistry Research*, *39*, 1596–1607.

Higler, A. P., Taylor, R., & Krishna, R. (1999). The influence of mass transfer and liquid mixing on the performance of reactive distillation tray column. *Chemical Engineering Science*, *54*, 2873–2881.

Kooijman, H. A. (1995). *Dynamic nonequilibrium column simulation*. Ph.D. dissertation, Clarkson University, Potsdam, USA.

Kooijman, H. A., & Taylor, R. (1995). A dynamic nonequilibrium model of tray distillation columns. *American Institute of Chemical Engineers Journal*, *41*, 1852–1863.

Kreul, L. U., Gorak, A., Dittrich, C., & Barton, P. I. (1998). Dynamic catalytic distillation: Advanced simulation and experimental validation. *Computers and Chemical Engineering*, *22*, S371–S378.

Krishna, R., & Wesselingh, J. A. (1997). The Maxwell-Stefan approach to mass transfer. *Chemical Engineering Science*, *52*, 861–911.

Kumar, A., & Daoutidis, P. (1999). Modeling, analysis and control of ethylene glycol reactive distillation column. *American Institute of Chemical Engineers Journal*, *45*, 51–68.

Moe, H. I., Hauan, S., Lien, K. M., & Hertzberg, T. (1995). Dynamic model of a system with phase and reaction equilibrium. *Computers and Chemical Engineering*, *19*, S513–S518.

Perez-Cisneros, E., Schenk, M., Gani, R., & Pilavachi, P. A. (1996). Aspects of simulation, design and analysis of reactive distillation operations. *Computers and Chemical Engineering*, *20*, S267–S272.

Roat, S. D., Downs, J. J., Vogel, E. F., & Doss, J. E. (1986). The integration of rigorous dynamic modeling and control system synthesis for distillation columns: An industrial approach. In M. Morari & T. J. McAvoy (Eds.), *Chemical process control – CPC III*. New York: Elsevier.

Ruiz, C. A., Basualdo, M. S., & Scenna, N. J. (1995). Reactive distillation dynamic simulation. *Chemical Engineering Research and Design, Transactions of the Institution of Chemical Engineers, Part A*, *73*, 363–378.

Scenna, N. J., Ruiz, C. A., & Benz, S. J. (1998). Dynamic simulation of startup procedures of reactive distillation columns. *Computers and Chemical Engineering*, *22*, S719–S722.

Schrans, S., de Wolf, S., & Baur, R. (1996). Dynamic simulation of reactive distillation, An MTBE case study. *Computers and Chemical Engineering*, *20* (Suppl.), S1619–S1624.

Sneesby, M. G., Tadé, M. O., & Smith, T. N. (1998). Steady-state transitions in the reactive distillation of MTBE. *Computers and Chemical Engineering*, *22*, 879–892.

Taylor, R., & Krishna, R. (1993). *Multicomponent mass transfer*. New York: Wiley.

Taylor, R., & Krishna, R. (2000). Modelling reactive distillation. *Chemical Engineering Science*, *55*, 5183–5229.